

# PROSPECT: Unified Streaming Vision-Language Navigation via Semantic–Spatial Fusion and Latent Predictive Representation

Zehua Fan<sup>1,\*</sup>, Wenqi Lyu<sup>3</sup>, Wenxuan Song<sup>5</sup>, Linge Zhao<sup>4</sup>, Yifei Yang<sup>6</sup>, Xi Wang<sup>7</sup>, Junjie He<sup>5</sup>, Lida Huang<sup>2</sup>, Haiyan Liu<sup>8</sup>, Bingchuan Sun<sup>8,◊</sup>, Guangjun Bao<sup>8</sup>, Xuanyao Mao<sup>8</sup>, Liang Xu<sup>8</sup>, Yan Wang<sup>2,◊</sup>, Feng Gao<sup>1,◊</sup>

**Abstract**—Multimodal large language models (MLLMs) have advanced zero-shot end-to-end Vision-Language Navigation (VLN), yet robust navigation requires not only semantic understanding but also predictive modeling of environment dynamics and spatial structure. We propose *PROSPECT*, a unified streaming navigation agent that couples a streaming Vision-Language-Action (VLA) policy with latent predictive representation learning. *PROSPECT* uses CUT3R as a streaming 3D foundation spatial encoder to produce long-context, absolute-scale spatial features, and fuses them with SigLIP semantic features via cross-attention. During training, we introduce learnable *stream query tokens* that query the streaming context and predict next-step 2D and 3D latent features (rather than pixels or explicit modalities), supervised in the latent spaces of frozen SigLIP and CUT3R teachers. The predictive branch shapes internal representations without inference overhead. Experiments on VLN-CE benchmarks and real-robot deployment demonstrate state-of-the-art performance and improved long-horizon robustness under diverse lighting. We will release code for the community soon.

**Index Terms**—Vision-language navigation, embodied AI, world models.

## I. INTRODUCTION

**V**ISION-LANGUAGE Navigation (VLN) is a key step toward general-purpose embodied agents. Recent multimodal large language models (MLLMs) enable strong zero-shot VLN by mapping egocentric observations to actions in a Vision-Language-Action (VLA) paradigm [1]–[4].

Nevertheless, strong navigation performance depends not only on understanding the world but also on predicting and generating future outcomes. World models address this by predicting future states from past context [5]–[9]. In VLA, unified frameworks that learn both action generation and predictive representations [10]–[12] can be more compact and synergistic than combining an MLLM with a separate video generator [13]–[15]. In navigation, existing predictive approaches either rely on low-dimensional state-space models with limited expressivity [16], or supervise in explicit pixel/depth spaces (concurrent work [17]), which may overfit to task-irrelevant details such as textures and illumination, degrading out-of-domain robustness. Many prior models condition on short history [12], [14], [15], underutilizing long streaming context.

Streaming VLN benefits from long-range context. StreamVLN [4] introduces a fast–slow context mechanism, but remains a VLA-only method without an explicit predictive component under streaming RGB.

The vision encoder also shapes downstream performance. Many VLN methods rely on 2D semantic encoders (e.g., SigLIP [18]) and thus lack spatial intelligence. Recent 3D foundation models (VGGT [19] and successors [20], [21], and CUT3R [22]) extract spatial features from RGB and are often fused with 2D features [23]–[25]. In VLN, a concurrent line of work explores VGGT as a spatial encoder [26]. VGGT-based encoders can be memory-heavy for long episodes and require ad-hoc history truncation to avoid out-of-memory (OOM) at inference. They also provide relative-scale representations, complicating the maintenance of consistency under large viewpoint changes. CUT3R is inherently streaming and yields absolute-scale spatial features, making it suited for long-context streaming navigation.

To address these limitations, we propose **PROSPECT** (**P**redictive **R**epresentations **O**f **S**patial-**s**EMantic **C**ontex**T**s), a unified architecture that combines streaming VLA with latent-space predictive representation learning, featuring long contextual semantics, spatial understanding, and predictive capabilities. *PROSPECT* takes streaming video and uses the streaming 3D foundation model (CUT3R) to continuously encode it into spatial features with absolute scale, which enhance 2D semantic features. Inspired by JEPA [5], [6], we predict future *latent* 2D/3D features rather than pixels/depth. We introduce *stream query tokens* to query the long streaming context and decode next-step 2D semantic and 3D spatial latent features during training. At inference, the predictive branch is removed; it has shaped the VLA representations to internalize dynamics without adding latency. Fig. 1 overviews the method.

Our contributions are:

- A unified streaming VLN framework that integrates streaming VLA with latent predictive representation learning, achieving first-tier VLN-CE performance.
- CUT3R-based streaming 3D perception with absolute-scale spatial features for efficient long-context navigation.
- Stream query tokens with a streaming-causal attention mask that enables latent prediction while disentangling 2D/3D objectives.
- Real-robot deployment demonstrating high-frequency control and robustness across indoor and outdoor scenes under diverse lighting conditions.

<sup>1</sup>Z. Fan and F. Gao are with Shanghai Jiao Tong University, Shanghai, China. <sup>2</sup>L. Huang and Y. Wang are with Tsinghua University, Beijing, China. <sup>3</sup>W. Lyu is with the University of Adelaide, Adelaide, Australia. <sup>4</sup>L. Zhao is with Wuhan University, Wuhan, China. <sup>5</sup>W. Song and J. He are with the Hong Kong University of Science and Technology (Guangzhou), Guangzhou, China. <sup>6</sup>Y. Yang is with Beijing Jiaotong University, Beijing, China. <sup>7</sup>X. Wang is with AIR Wuxi Innovation Center, Tsinghua University, Wuxi, China. <sup>8</sup>H. Liu, B. Sun, G. Bao, X. Mao, and L. Xu are with Lenovo, Beijing, China. ◊ Corresponding authors: Yan Wang, Bingchuan Sun and Feng Gao.

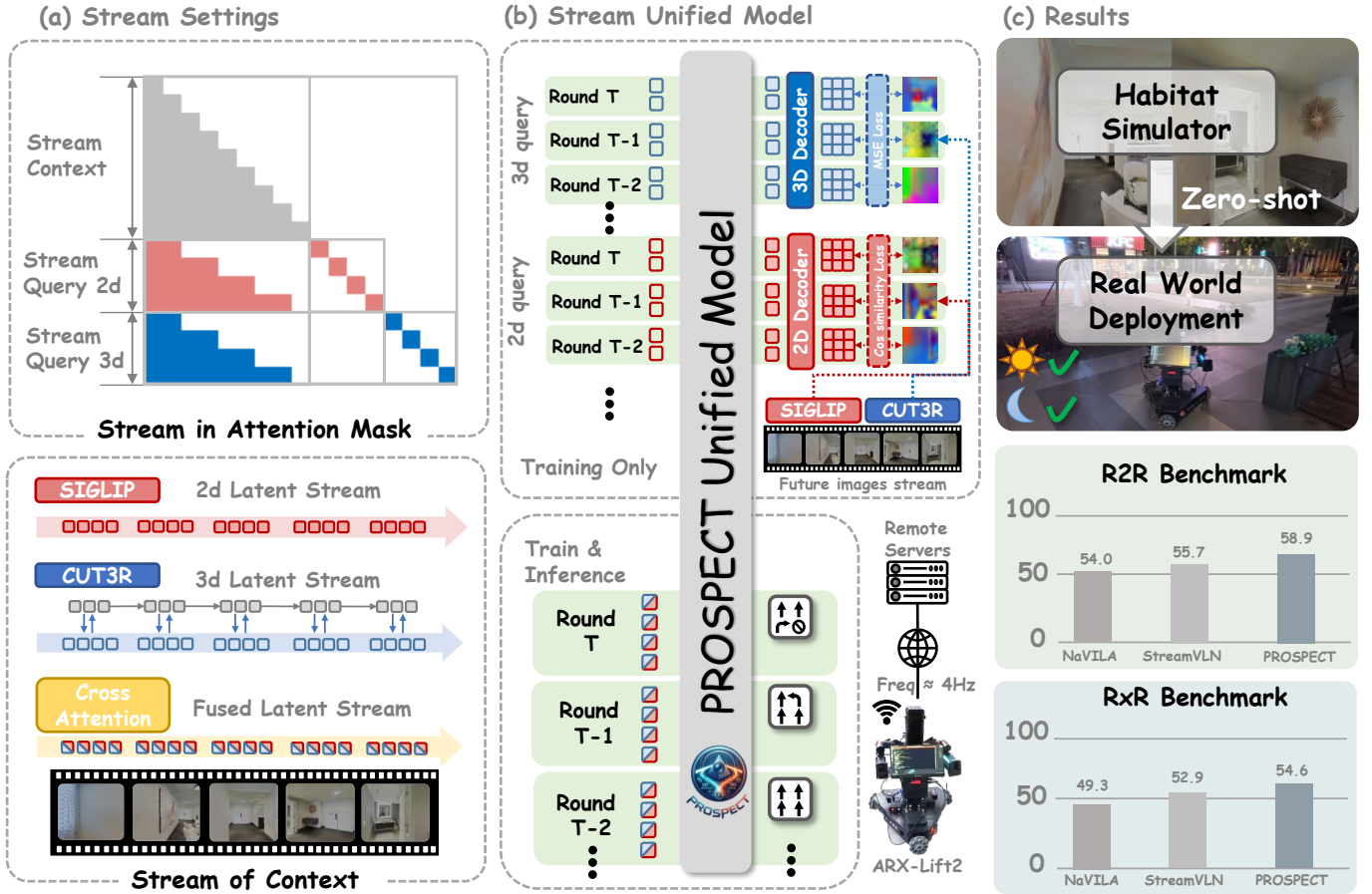


Fig. 1. Overview of PROSPECT. (a) **Streaming setup**: A streaming attention mask enforces temporal causality and isolates 2D/3D query tokens to prevent cross-modal leakage. SigLIP and CUT3R provide 2D semantic and absolute-scale 3D spatial feature streams, fused by cross-attention for the policy. (b) **Unified model**: In training, stream query tokens predict next-step 2D/3D latent features under frozen SigLIP/CUT3R supervision (no inference cost). At inference, only the VLA policy runs at  $\sim 4$ Hz. (c) **Results**: First-tier VLN-CE performance and zero-shot Habitat navigation; larger gains on the long-horizon RxR benchmark than on R2R, indicating stronger robustness for complex instruction following. Real-robot deployment is robust under diverse lighting.

## II. RELATED WORKS

### A. Embodied Navigation

Embodied navigation spans Vision Navigation (VN) and VLN. Earlier VLN systems established benchmarks and reliable continuous-environment protocols [27]–[34]. With MLLMs and VLA models, approaches represented by NaVid advance end-to-end navigation from egocentric RGB without odometry or pre-built maps [1]–[4], [35]. Nevertheless, they primarily emphasize action generation and language grounding, leaving spatial understanding and future prediction capability underexplored in a unified streaming setting. We propose a unified streaming VLN paradigm that couples spatial understanding with latent predictive representation learning via stream query tokens, yielding an end-to-end agent that handles long-context streams, maintains spatial grounding, and remains prediction-shaped.

### B. World Models and Predictive Representations

World models are often framed as future frame generators [8], [36], and in embodied settings extend to explicit modalities (BEV/occupancy/depth/segmentation) [12], [17],

[37], [38]. Supervision in explicit spaces can overweight task-irrelevant appearance factors. In contrast, motivated by JEPa [5], [6], we supervise prediction directly in compact latent spaces of 2D semantics and 3D spatial features, encouraging dynamics-aware representations without modeling pixel noise.

In VLN, few works combine future frame or latent feature prediction with navigation [16], [17]; they often omit 3D fusion or depend on simulator-provided poses and ground-truth states, thereby limiting mapless and odometry-free deployment. PROSPECT unifies streaming updates, 2D–3D fusion, and latent prediction in an end-to-end framework.

### C. Spatial Intelligence

Spatial intelligence concerns representing and reasoning about 3D structure [39], [40]. Representations include depth/point clouds, 3D Gaussians [41], BEV/occupancy [37], [38], and 3D foundation features [19]–[22], [42]. 3D foundation features are compact and effective in VLA settings [23], [24]. We adopt CUT3R for its inherent streaming capability and absolute-scale spatial representations, which enable stable long-context VLN.

### III. METHOD

#### A. Problem Formulation: Streaming VLA for VLN

Streaming VLN can be formulated as a streaming VLA problem. Given a language instruction  $I$ , at each time step  $t$  the agent receives an observation  $o_t$  and produces an action  $a_t$ , interacting with the environment in an alternating perception–action stream [4]. Let  $\mathcal{W}_t = \{o_{t-N+1}, a_{t-N+1}, \dots, o_{t-1}, a_{t-1}\}$  denote the  $N-1$  preceding observation–action pairs in the  $N$  step sliding window. The streaming context is:

$$\text{Stream}_{0:t} := \{ \text{KV}(\mathcal{W}_t), o_t, M \}, \quad (1)$$

where  $\text{KV}(\cdot)$  caches the key–value states of the short-term sliding window, and  $M$  is long-term memory tokens summarizing uniformly sampled historical keyframes.

In mapless, odometry-free VLN,  $o_t \in \mathbb{R}^{3 \times H \times W}$  is a single-view RGB image. We use standard atomic actions [1], [4]: the model outputs  $n_a$  actions per step,  $a_t = (a_t^{(1)}, \dots, a_t^{(n_a)})$  with  $n_a = 4$ , where

$$a_t^{(i)} \in \mathcal{A} := \{\uparrow, \leftarrow, \rightarrow, \text{STOP}\}. \quad (2)$$

Here  $\uparrow$  is moving forward 25 cm and  $\leftarrow / \rightarrow$  are turning 15° left/right. The streaming policy is

$$a_t = \text{VLA}(I, \text{Stream}_{0:t}). \quad (3)$$

#### B. Unified Streaming Navigation with Latent Prediction

Temporal correlations among semantics, spatial layout, physical dynamics, and task progress are rich yet implicit. Next-frame prediction is naturally compatible with streaming and can benefit from scaling, while improving physical understanding. We thus propose a unified streaming model that produces both navigation actions and future latent features:

$$a_t, \mathbf{F}_{t+1}^{2D}, \mathbf{F}_{t+1}^{3D} = \text{UM}(I, \text{Stream}_{0:t}), \quad (4)$$

where  $\text{UM}(\cdot)$  denotes PROSPECT, and  $\mathbf{F}_{t+1}^{2D}/\mathbf{F}_{t+1}^{3D}$  are predicted 2D semantic / 3D spatial latent features.

Fig. 2 shows the architecture. The VLA branch encodes fused 2D–3D features and autoregressively outputs actions. During training, the predictive branch appends time-ordered query tokens that attend to the streaming context; lightweight decoders then predict next-step latent features. Understanding and generation are unified in one streaming framework.

#### C. Perception and Representation: 2D–3D Fusion

SigLIP encodes each observation into 2D semantic features:

$$\mathbf{F}_t^{2D} = \text{SigLIP}(o_t). \quad (5)$$

For spatial features, we use CUT3R as a streaming 3D encoder. CUT3R first encodes the frame by a ViT encoder,

$$\mathbf{F}_t^{3D,\text{pre}} = \text{Encoder}(o_t). \quad (6)$$

With a previous state token  $\mathbf{s}_{t-1}$ , a learnable pose token  $\mathbf{p}_t$ , and current features  $\mathbf{F}_t^{3D,\text{pre}}$ , the decoder rolls out spatial features and updates the state:

$$[\mathbf{p}'_t, \mathbf{F}_t^{3D}], \mathbf{s}_t = \text{Decoders}([\mathbf{p}_t, \mathbf{F}_t^{3D,\text{pre}}], \mathbf{s}_{t-1}). \quad (7)$$

We fuse  $\mathbf{F}_t^{2D}$  and  $\mathbf{F}_t^{3D}$  via cross-attention:

$$\mathbf{F}_t^{\text{fuse}} = \text{softmax}\left(\frac{(\mathbf{F}_t^{2D}\mathbf{W}_Q)(\mathbf{F}_t^{3D}\mathbf{W}_K)^\top}{\sqrt{d_k}}\right)(\mathbf{F}_t^{3D}\mathbf{W}_V), \quad (8)$$

where  $d_k$  is the key dimension and  $\mathbf{W}_Q, \mathbf{W}_K, \mathbf{W}_V$  are learnable projections. Each  $\mathbf{F}_t^{\text{fuse}}$  is then mapped through an MLP into the LLM embedding space and fed to the LLM along with instruction tokens. The historically sampled keyframes that form long-term memory  $M$  are encoded with the same 2D–3D fusion pipeline; each keyframe’s fused representation is condensed into a single token before being fed to the LLM.

#### D. Latent Prediction via Stream Query Tokens

While fused 2D–3D features provide a *forward* aggregation of streaming information into the LLM, we introduce stream query tokens to *reverse-query* the streaming context and predict future latent features. At step  $t$ , we append learnable tokens  $\langle q_t^{2D} \rangle$  and  $\langle q_t^{3D} \rangle$  to the LLM input, yielding compact embeddings of the future time step  $t+1$ :

$$\mathbf{e}_{t+1}^{2D} = \text{LLM}(I, \text{Stream}_{0:t} \mid \langle q_t^{2D} \rangle), \quad (9)$$

$$\mathbf{e}_{t+1}^{3D} = \text{LLM}(I, \text{Stream}_{0:t} \mid \langle q_t^{3D} \rangle). \quad (10)$$

Two lightweight Transformer decoders reconstruct token-level latent features from these embeddings:

$$\widehat{\mathbf{F}}_{t+1}^{2D} = \text{Decoder}_{2D}(\mathbf{e}_{t+1}^{2D} \mid \langle m_t^{2D} \rangle), \quad (11)$$

$$\widehat{\mathbf{F}}_{t+1}^{3D} = \text{Decoder}_{3D}(\mathbf{e}_{t+1}^{3D} \mid \langle m_t^{3D} \rangle), \quad (12)$$

where  $\langle m_t^{2D} \rangle$  and  $\langle m_t^{3D} \rangle$  are learnable masked tokens repeated to match the target token length. Each decoder has 2 layers and predicts a full-length latent sequence aligned with the target image-token sequence.

Targets  $\mathbf{F}_{t+1}^{2D}$  and  $\mathbf{F}_{t+1}^{3D}$  are computed from the next-step observation using frozen SigLIP and CUT3R teachers (no gradient). We supervise 2D with cosine distance and 3D with MSE:

$$\mathcal{L}_{2D} = 1 - \cos\left(\widehat{\mathbf{F}}_{t+1}^{2D}, \mathbf{F}_{t+1}^{2D}\right), \quad (13)$$

$$\mathcal{L}_{3D} = \text{MSE}\left(\widehat{\mathbf{F}}_{t+1}^{3D}, \mathbf{F}_{t+1}^{3D}\right). \quad (14)$$

SigLIP is trained with a pairwise sigmoid loss on  $\ell_2$ -normalized embeddings. In our experiments, cosine loss aligns well with this normalized geometry, whereas applying MSE to 2D features penalizes norm differences and leads to unstable training; in contrast, MSE was stable for CUT3R features.

The overall objective is

$$\mathcal{L}_{\text{all}} = \mathcal{L}_{\text{nav}} + \gamma(\alpha \mathcal{L}_{2D} + \beta \mathcal{L}_{3D}), \quad (15)$$

where  $\mathcal{L}_{\text{nav}}$  is action cross-entropy [4] and  $(\gamma, \alpha, \beta)$  are set in Sec. IV.

#### E. Streaming Attention Mask

A standard causal mask is insufficient because we introduce per-step predictive queries. We interpret the short-term navigation context as an  $N$ -turn dialogue: at each turn  $i$ , the model consumes context  $\text{ctx}_i$  (prompt and observation tokens) and produces a response  $\text{act}_i$  (actions). The initial turn includes

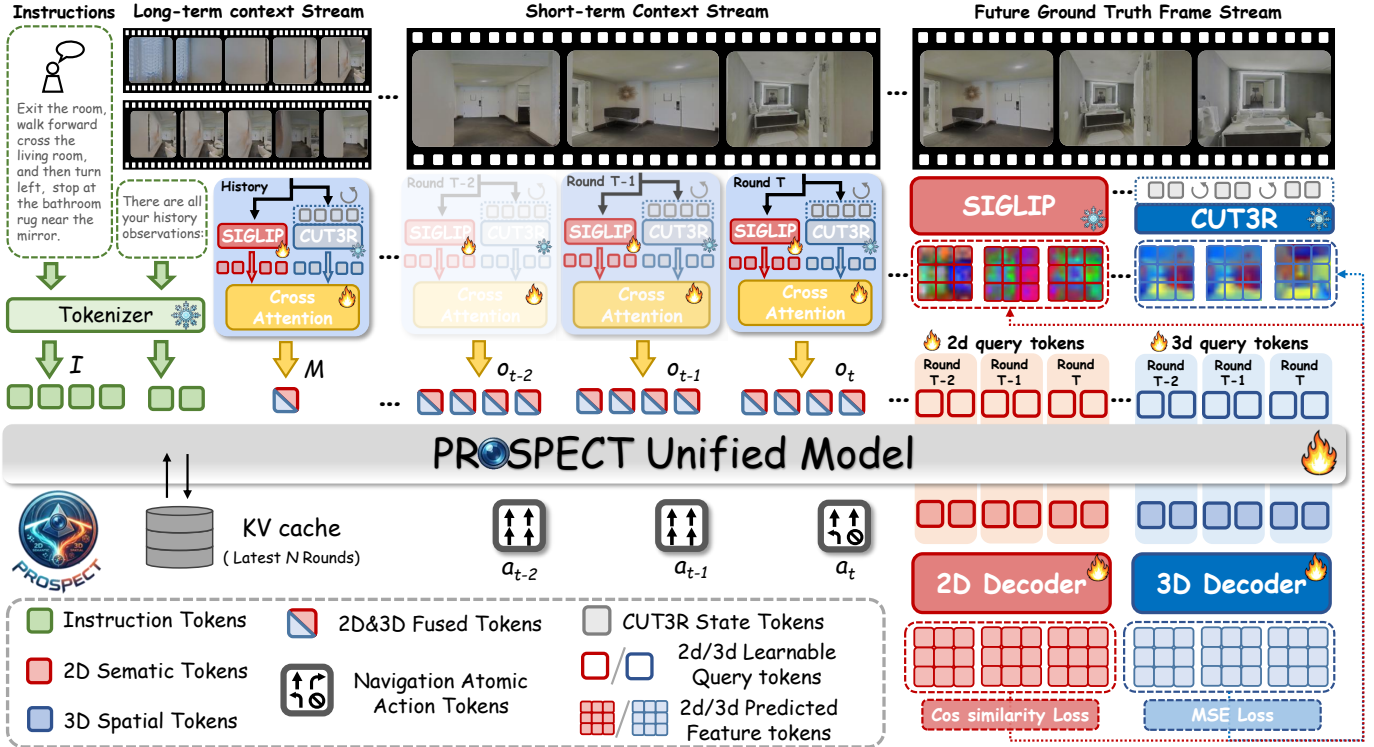


Fig. 2. Architecture of PROSPECT. Instruction and observations (historical keyframes and current frame) share one pipeline: frozen SigLIP and CUT3R with cross-attention fusion; keyframes are condensed into long-term memory  $M$ . The model uses a KV cache for context and autoregressively outputs navigation actions. Training only: 2D/3D query tokens reverse-query the stream; lightweight decoders predict next-step latents under cosine (2D) and MSE (3D) with frozen teachers. Predictive branch removed at inference.

the instruction and long-term memory  $M$ . During training, we augment each turn by appending  $\langle q_i^{2D} \rangle$  and  $\langle q_i^{3D} \rangle$  to the end of the input sequence.

We enforce three constraints for correct causality, learning efficiency, and train–test alignment in the unified streaming model. First, for causality, each query token attends only to its own turn and all previous turns, never to future turns. Second, to avoid leakage and reduce error accumulation, query tokens from different turns are isolated (no mutual attention), so each query extracts information only from the shared streaming context rather than from other queries. Third, to disentangle modality-specific supervision, 2D and 3D queries are mutually masked and cannot attend to each other, reducing cross-task interference and preventing degenerate information mixing. During evaluation, we remove the query-token prediction branch; the remaining token sequence preserves the same relative ordering and attention structure as in training, ensuring inference efficiency and effective use of the prediction-shaped representations learned during training. Fig. 3 illustrates the mask.

## IV. EXPERIMENTAL SETUP

### A. Datasets and Training Settings

We adopt StreamVLN [4] as baseline and use LLaVA-NeXT-Video-7B with a Qwen1.5-7B LLM [43]. Following [4], we set short-term window  $N = 8$  and sample 8 long-

term keyframes for  $M$ . Training uses  $8 \times$  A800 GPUs in two stages.

**Stage 1 (SFT).** One-epoch supervised fine-tuning on VLN-CE data in Matterport3D (MP3D): R2R [44], RxR [45], and R2R-EnvDrop [46] (total  $\sim 479$ K; R2R/RxR/EnvDrop contribute  $\sim 5\%/\sim 14\%/\sim 80\%$ ). One epoch costs 560 A800 GPU-hours.

**Stage 2 (Augmented SFT).** We retain the Stage 1 R2R/RxR trajectories to mitigate forgetting, and add  $\sim 260$ K DAGger samples [47], where expert relabeling provides recovery actions for off-policy deviations, as well as  $\sim 314$ K ScaleVLN samples [48], [49], a large-scale VLN dataset in Habitat Matterport3D (HM3D). To encourage multimodal and spatial reasoning, we mix in VQA data targeting video-based spatial and geometric understanding, including LLaVA-Video-178K [50] and ScanQA [51]. Stage 2 mixture contains  $\sim 938$ K samples (71% VLN, 29% VQA), and one epoch costs  $\sim 1900$  A800 GPU-hours.

We set the learning rate to  $5 \times 10^{-6}$  for SigLIP and use a peak  $2 \times 10^{-5}$  for all other trainable modules; CUT3R is frozen. Warm-up ratios are 7.5% (Stage 1) and 3% (Stage 2). We set  $\gamma = 0.01$ ,  $\alpha = 0.25$ , and  $\beta = 0.75$  to balance the loss scales, preventing any single term from dominating due to magnitude alone. We use 196 masked tokens and 9 query tokens per modality, trading off representation capacity, the LLM input token budget, and compute cost.

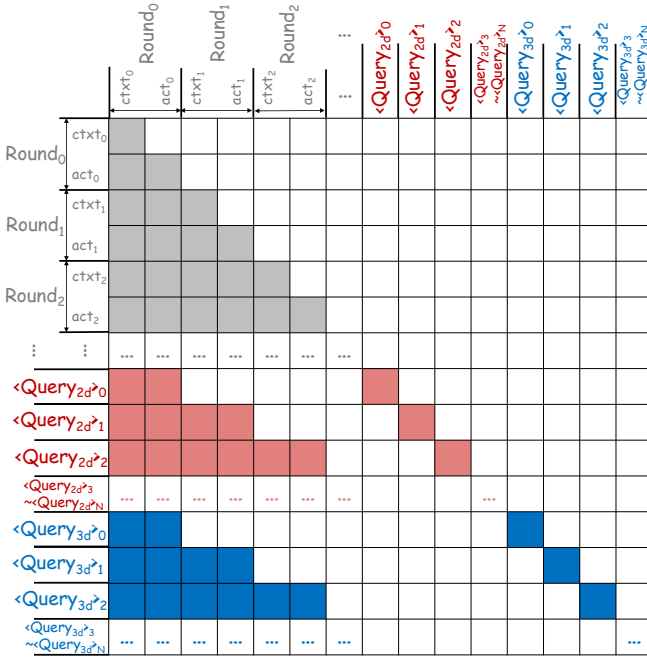


Fig. 3. Streaming attention mask used by PROSPECT. **Upper (gray):** Causal mask for navigation context (ctxt) and actions (act): each  $act_i$  may attend only to  $ctxt_{0:i}$  and  $act_{0:i-1}$ , ensuring no future leakage. **Middle (red):** Each 2D query token ( $\langle \text{Query}_{2d} \rangle_i$ ) attends only to its own round and prior rounds’  $ctxt/act$ ; it cannot attend to any other  $\text{Query}_{2d}$ , any  $\text{Query}_{3d}$ , or future rounds—enforcing both turn isolation and modality disentanglement. **Lower (blue):** Same for 3D query tokens ( $\langle \text{Query}_{3d} \rangle_i$ ).

## B. Benchmarks and Metrics

We evaluate on VLN-CE in Habitat [52], reporting Success Rate (SR), Success weighted by Path Length (SPL), Navigation Error (NE), and Oracle Success Rate (OSR) on the val-unseen split of R2R and RxR [44], [45].

### C. Real-Robot Deployment

We deploy on an ARX-Lift2 robot using egocentric RGB from a head-mounted RealSense 405. As in most prior VLN robot deployments [1], [4], we run remote inference over Wi-Fi/LAN indoors (dual RTX-4090 server;  $\sim 0.25$  s/step,  $\sim 4$  Hz) and over public network outdoors (dual A800 server;  $\sim 0.27$  s/step,  $\sim 4$  Hz) with authenticated access. We also test onboard inference on a single RTX 4070 with reduced precision; success is lower but remains feasible for less demanding scenarios.

## V. EXPERIMENTS

### A. Main Results on VLN-CE Benchmarks

Table I compares PROSPECT with prior methods on VLN-CE R2R/RxR val-unseen under controlled training-data regimes for fair comparison. PROSPECT uses single-view RGB per step (no depth, odometry, or panoramic inputs) and achieves first-tier performance both with MP3D-only navigation data and with scaled training that includes non-MP3D data (e.g., ScaleVLN). Our performance gains on RxR val-unseen are substantially larger than those on R2R

(Table I). RxR contains twice as many evaluation episodes as R2R, with a longer average trajectory length (15.32 m vs. 9.89 m, i.e.,  $1.55\times$ ), and markedly longer instructions (about 120 words on average versus 32, nearly  $4\times$ ). RxR is widely regarded as a more long-horizon and challenging benchmark; the larger improvements on RxR show that the proposed paradigm is particularly beneficial for long-horizon instruction-following navigation.

### B. Ablations

1) *Module Ablation:* We ablate PROSPECT on R2R/RxR/R2R-EnvDrop under one-epoch SFT, with SigLIP-only as the baseline. Table II shows that SigLIP-CUT3R fusion consistently improves performance, and adding either the 2D or 3D latent prediction objective yields additional gains in SR/SPL. Combining both objectives achieves the best result (SR 48.7, SPL 42.9), indicating complementary semantic and geometric predictive signals that jointly provide stronger inductive bias for navigation.

2) *Spatial Encoder Choice: CUT3R vs. (Infinite)VGGT:* We compare CUT3R with VGGT-style spatial encoders under one-epoch SFT on R2R/RxR/EnvDrop and evaluation on R2R val-unseen. VGGT often OOMs on long R2R episodes (most exceed 30 frames), so we use InfiniteVGGT as the strongest streaming VGGT baseline. Table III shows CUT3R achieves better accuracy and lower latency, which we attribute to its absolute-scale spatial representation versus first-frame-relative scale in VGGT-style encoders.

3) *Task Complexity: Short vs. Medium vs. Long Horizon:* We stratify R2R val-unseen by executed steps: short (1–50), medium (50–100), long ( $\geq 100$ ). Table IV shows that PROSPECT matches baseline on short tasks and yields larger improvements on medium and long tasks, indicating stronger generalization under long streaming context.

4) *Ablation on Query Attention Mask Design:* To validate our query attention mask design, we conduct ablations on three variants evaluated on R2R val-unseen. **Ours** enforces strict causal masking and full 2D/3D query isolation, preventing each query from attending to future navigation tokens or queries of a different modality. **w/o Isolation** retains the causal constraint but allows 2D and 3D queries within the same round to attend each other, introducing cross-modal feature entanglement. **Leaky** applies a standard causal mask without isolation, enabling queries to implicitly access future navigation tokens and causing information leakage during training. Results in Table V confirm that both isolation and causal strictness are essential for robust navigation performance.

### C. Real-Robot Results

We evaluate on ARX-Lift2 across indoor/outdoor scenes with varying illumination. Per scene, we group episodes into short/medium/long horizons by the number of executed steps ( $< 50$ ,  $[50, 100)$ , and  $\geq 100$ ). For each horizon, we design five distinct instructions and execute each instruction twice, resulting in 30 trials per scene. All real-world scenes are unseen during training; we select goal locations and trajectories to cover diverse layouts and visual appearances

TABLE I  
COMPARISON WITH STATE-OF-THE-ART METHODS ON VLN-CE R2R AND R2R VAL-UNSEEN SPLIT.

Method	Obs. Enc.				R2R Val-Unseen				RxR Val-Unseen			
	Pano.	Odo.	D.	S.RGB	NE↓	OSR↑	SR↑	SPL↑	NE↓	SR↑	SPL↑	nDTW↑
HPN+DN [ICCV21] [27]	✓	✓	✓	–	6.31	40.0	36.0	34.0	–	–	–	–
CMA [CVPR22] [28]	✓	✓	✓	–	6.20	52.0	41.0	36.0	8.76	26.5	22.1	47.0
VLN $\odot$ BERT [CVPR22] [28]	✓	✓	✓	–	5.74	53.0	44.0	39.0	8.98	27.0	22.6	46.7
Sim2Sim [ECCV22] [29]	✓	✓	✓	–	6.07	52.0	43.0	36.0	–	–	–	–
GridMM [ICCV23] [30]	✓	✓	✓	–	5.11	61.0	49.0	41.0	–	–	–	–
InstructNav [arXiv24] [32]	–	–	–	–	6.89	–	31.0	24.0	–	–	–	–
AG-CMTP [CVPR21] [33]	✓	✓	✓	–	7.90	39.2	23.1	19.1	–	–	–	–
R2R-CMTP [CVPR21] [33]	✓	✓	✓	–	7.90	38.0	26.4	22.7	–	–	–	–
LAW [EMNLP21] [53]	–	✓	–	✓	6.83	44.0	35.0	31.0	10.90	8.0	8.0	38.0
CM2 [CVPR22] [54]	–	✓	✓	✓	7.02	41.5	34.3	27.6	–	–	–	–
WS-MGMap [NeurIPS22] [55]	–	✓	✓	✓	6.28	47.6	38.9	34.3	–	–	–	–
ETPNav+FF [arXiv24] [34]	–	✓	✓	✓	5.95	55.8	44.9	30.4	8.79	25.5	18.1	–
Seq2Seq [ECCV20] [52]	–	–	✓	✓	7.77	37.0	25.0	22.0	12.10	13.9	11.9	30.8
CMA [ECCV20] [52]	–	–	✓	✓	7.37	40.0	32.0	30.0	–	–	–	–
NavMorph [ICCV25] [16]	–	–	✓	✓	5.75	56.9	47.9	33.2	8.85	30.8	22.8	44.2
NaVid [RSS24] [1]	–	–	–	✓	5.47	49.1	37.4	35.9	–	–	–	–
Uni-Navid [RSS25] [2]	–	–	–	✓	5.58	53.3	47.0	42.7	6.24	48.7	40.9	–
NaVILA [RSS25] [3]	–	–	–	✓	5.37	57.6	49.7	45.5	–	–	–	–
StreamVLN* [arXiv25] [4]	–	–	–	✓	5.47	57.8	50.8	45.7	6.72 <sup>‡</sup>	48.6 <sup>‡</sup>	42.5 <sup>‡</sup>	60.2 <sup>‡</sup>
<b>PROSPECT (Ours)*</b>	–	–	–	✓	5.31	60.3	52.0	46.2	5.93	52.7	42.8	60.6
NaVILA <sup>†</sup> [RSS25] [3]	–	–	–	✓	5.22	62.5	54.0	49.0	6.77	49.3	44.0	58.8
StreamVLN <sup>†</sup> [arXiv25] [4]	–	–	–	✓	5.10	64.0	55.7	50.9	6.22	52.9	46.0	61.9
<b>PROSPECT (Ours)<sup>†</sup></b>	–	–	–	✓	<b>4.92</b>	<b>65.2</b>	<b>58.9</b>	<b>54.0</b>	<b>5.70</b>	<b>54.6</b>	<b>46.2</b>	<b>62.1</b>

Note. Obs. Enc.: Pano.=panoramic, Odo.=odometry, D.=depth, S.RGB=single-view RGB.

\*: MP3D + VideoQA only (StreamVLN [4] Table 3 row 2).

†: Non-MP3D and Extra data: Ours and StreamVLN add ScaleVLN and MMC4 ([4] Table 3 row 4); NaVILA adds human-following data.

‡: RxR under \* not reported by StreamVLN; we quote their numbers from a recipe that adds MMC4 on top of \* for reference ([4] Table 1 row 20).

TABLE II  
MODULE ABLATION ON R2R VAL-UNSEEN.

Setting	NE↓	OSR↑	SR↑	SPL↑
Baseline (SigLIP only)	6.05	53.8	45.5	41.6
Ours (SigLIP + CUT3R)	5.91	55.0	46.7	41.8
Ours (+ WM-2D only)	5.89	56.0	47.0	42.0
Ours (+ WM-3D only)	5.90	55.4	47.2	41.9
<b>Ours (+ WM-2D + WM-3D)</b>	<b>5.82</b>	<b>57.6</b>	<b>48.7</b>	<b>42.9</b>

TABLE III  
SPATIAL ENCODER ABLATION ON R2R VAL-UNSEEN.

Encoder	Time (s)	SR ↑	SPL ↑	OSR ↑	NE ↓
VGGT [19]	OOM	OOM	OOM	OOM	OOM
InfiniteVGGT [21]	0.284	43.2	38.0	54.4	6.61
<b>Ours (CUT3R) [22]</b>	<b>0.245</b>	<b>48.7</b>	<b>42.9</b>	<b>57.6</b>	<b>5.82</b>

(e.g., texture, clutter, illumination) and varying instruction complexity. Success requires reaching within 0.3 m of the goal within 500 steps and outputting STOP; collisions count as failures. The indoor trials are under ceiling lighting and are well-lit; the outdoor trials span afternoon, dusk, and night.

Table VI shows PROSPECT improves over NaVid and StreamVLN across scenes and lighting. Fig. 4 visualizes example runs; additional results appear in the supplementary video.

## VI. CONCLUSION

We presented PROSPECT, a unified streaming VLN agent integrating streaming VLA, CUT3R-based absolute-scale 3D

TABLE IV  
PERFORMANCE BY TASK HORIZON ON R2R VAL-UNSEEN.

Horizon	Model	#Ep	SR ↑	SPL ↑	OSR ↑	NE ↓
Short (1–50)	Baseline	459	51.20	48.18	55.34	5.08
	Ours	486	51.23	48.84	54.53	4.86
	<b>Difference</b>	<b>+27</b>	<b>+0.03</b>	<b>+0.66</b>	<b>-0.81</b>	<b>-0.22</b>
Medium (50–100)	Baseline	1038	49.61	43.79	61.27	5.64
	Ours	1061	54.29	48.04	63.71	5.46
	<b>Difference</b>	<b>+23</b>	<b>+4.68</b>	<b>+4.25</b>	<b>+2.44</b>	<b>-0.18</b>
Long (≥100)	Baseline	342	20.18	10.61	34.21	9.11
	Ours	292	24.32	14.25	40.75	8.74
	<b>Difference</b>	<b>-50</b>	<b>+4.14</b>	<b>+3.64</b>	<b>+6.54</b>	<b>-0.37</b>
Overall	Baseline	1839	44.54	38.72	54.76	6.15
	Ours	1839	48.72	42.88	57.64	5.82
	<b>Difference</b>	<b>0</b>	<b>+4.18</b>	<b>+4.16</b>	<b>+2.88</b>	<b>-0.33</b>

Note. “#Ep” denotes the number of episodes in each horizon for each model.

TABLE V  
ABLATION ON ATTENTION MASK DESIGN ON R2R VAL-UNSEEN.

Mask Design	NE↓	OSR↑	SR↑	SPL↑
Leaky	6.81	51.3	40.2	35.7
w/o Isolation	6.98	51.1	39.9	35.3
<b>Ours</b>	<b>5.82</b>	<b>57.6</b>	<b>48.7</b>	<b>42.9</b>

encoding, and latent predictive representation learning via stream query tokens. The predictive branch is used only during training to shape representations without inference overhead. PROSPECT achieves first-tier VLN-CE performance and robust real-robot navigation under diverse lighting. Future work will explore further refinements to robustness and efficiency in real-world deployments.

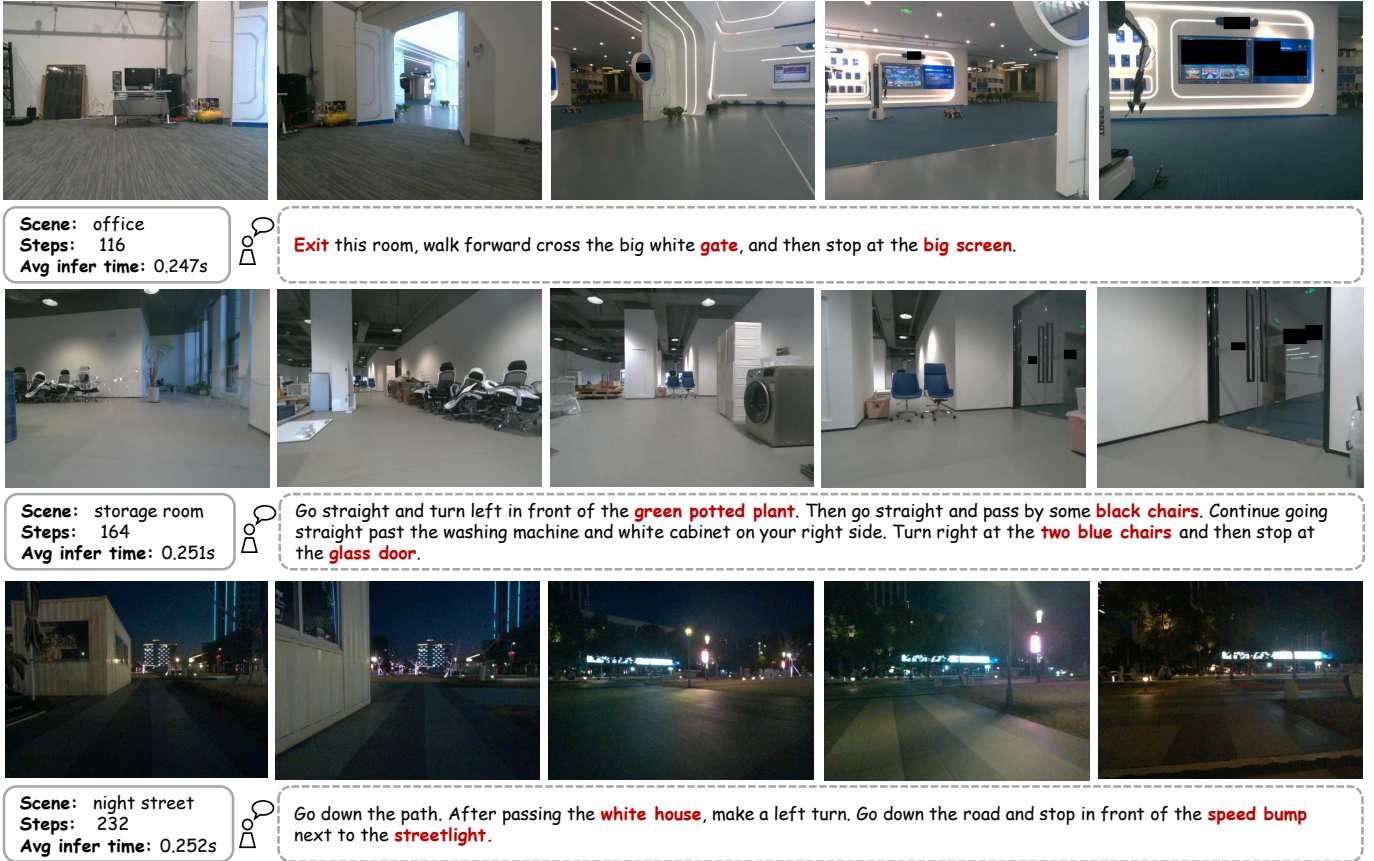


Fig. 4. First-person views from ARX-Lift2 under diverse indoor/outdoor lighting.

TABLE VI  
REAL-ROBOT SUCCESS RATES (COMPLETED/TOTAL) BY SCENE AND LIGHTING.

Scene	Lighting	NaVid [1]	StreamVLN [4]	Ours
<i>Indoor</i>				
Office	Bright	7/30	12/30	<b>20/30</b>
Warehouse	Bright	6/30	12/30	<b>18/30</b>
Corridor	Moderate	11/30	16/30	<b>22/30</b>
<i>Outdoor</i>				
Afternoon	Bright	6/30	10/30	<b>18/30</b>
Dusk	Moderate	4/30	6/30	<b>11/30</b>
Night Street	Low	2/30	6/30	<b>9/30</b>

## REFERENCES

- [1] J. Zhang, K. Wang, R. Xu, G. Zhou, Y. Hong, X. Fang, Q. Wu, Z. Zhang, and H. Wang, "Navid: Video-based VLM plans the next step for vision-and-language navigation," *arXiv preprint arXiv:2402.15852*, 2024.
- [2] J. Zhang, K. Wang, S. Wang, M. Li, H. Liu, S. Wei, Z. Wang, Z. Zhang, and H. Wang, "Uni-navid: A video-based vision-language action model for unifying embodied navigation tasks," *arXiv preprint arXiv:2412.06224*, 2024.
- [3] A.-C. Cheng, Y. Ji, Z. Yang, Z. Gongye, X. Zou, J. Kautz, E. Bityk, H. Yin, S. Liu, and X. Wang, "Navila: Legged robot vision-language action model for navigation," *arXiv preprint arXiv:2412.04453*, 2024.
- [4] M. Wei, C. Wan, X. Yu, T. Wang, Y. Yang, X. Mao, C. Zhu, W. Cai, H. Wang, Y. Chen *et al.*, "Streamvln: Streaming vision-and-language navigation via slowfast context modeling," *arXiv preprint arXiv:2507.05240*, 2025.
- [5] M. Assran, Q. Duval, I. Misra, P. Bojanowski, P. Vincent, M. Rabbat, Y. LeCun, and N. Ballas, "Self-supervised learning from images with a joint-embedding predictive architecture," in *Proceedings of the IEEE/CVF conference on computer vision and pattern recognition*, 2023, pp. 15 619–15 629.
- [6] M. Assran, A. Bardes, D. Fan, Q. Garrido, R. Howes, M. Muckley, A. Rizvi, C. Roberts, K. Sinha, A. Zhohus *et al.*, "V-jepa 2: Self-supervised video models enable understanding, prediction and planning," *arXiv preprint arXiv:2506.09985*, 2025.
- [7] X. Wang, X. Zhang, Z. Luo, Q. Sun, Y. Cui, J. Wang, F. Zhang, Y. Wang, Z. Li, Q. Yu *et al.*, "Emu3: Next-token prediction is all you need," *arXiv preprint arXiv:2409.18869*, 2024.
- [8] T. Wan, A. Wang, B. Ai, B. Wen, C. Mao, C.-W. Xie, D. Chen, F. Yu, H. Zhao, J. Yang *et al.*, "Wan: Open and advanced large-scale video generative models," *arXiv preprint arXiv:2503.20314*, 2025.
- [9] A. Bar, G. Zhou, D. Tran, T. Darrell, and Y. LeCun, "Navigation world models," in *Proceedings of the Computer Vision and Pattern Recognition Conference*, 2025, pp. 15 791–15 801.
- [10] J. Cen *et al.*, "Worldvla: Towards autoregressive action world model," 2025, arXiv:2506.21539.
- [11] J. Cen, S. Huang, Y. Yuan, C. Yu, Y. Jiang, J. Guo, K. Li, H. Luo, F. Wang, X. Li, D. Zhao, and H. Chen, "Rynnvla-002: A unified vision-language-action and world model," 2025, arXiv:2511.17502.
- [12] W. Zhang, H. Liu, Z. Qi, Y. Wang, X. Yu, J. Zhang, R. Dong, J. He, F. Lu, H. Wang, Z. Zhang, L. Yi, W. Zeng, and X. Jin, "Dreamvla: A vision-language-action model dreamed with comprehensive world knowledge," 2025, arXiv:2507.04447.
- [13] X. Pan, S. N. Shukla, A. Singh, Z. Zhao, S. K. Mishra, J. Wang, Z. Xu, J. Chen, K. Li, F. Juefei-Xu *et al.*, "Transfer between modalities with metaqueries," *arXiv preprint arXiv:2504.06256*, 2025.
- [14] Y. Yang, X. Li, Y. Chen, J. Song, Y. Wang, Z. Xiao, J. Su, Q. You, P. Liu, and Z. Deng, "Mantis: A versatile vision-language-action model with disentangled visual foresight," 2025, arXiv:2511.16175.
- [15] H. Bi, H. Tan, S. Xie, Z. Wang, S. Huang, H. Liu, R. Zhao, Y. Feng, C. Xiang, Y. Rong, H. Zhao, H. Liu, Z. Su, L. Ma, H. Su, and J. Zhu, "Motus: A unified latent action world model," 2025, arXiv:2512.13030.
- [16] X. Yao, J. Gao, and C. Xu, "Navmorph: A self-evolving world model for vision-and-language navigation in continuous environments," in

- Proceedings of the IEEE/CVF International Conference on Computer Vision*, 2025, pp. 5536–5546.
- [17] F. Liu, S. Xie, M. Luo, Z. Chu, J. Hu, X. Wu, and M. Xu, “Navforesee: A unified vision-language world model for hierarchical planning and dual-horizon navigation prediction,” *arXiv preprint arXiv:2512.01550*, 2025.
- [18] M. Tschannen, A. Gritsenko, X. Wang, M. F. Naeem, I. Alabdulmohsin, N. Parthasarathy, T. Evans, L. Beyler, Y. Xia, B. Mustafa *et al.*, “Siglip 2: Multilingual vision-language encoders with improved semantic understanding, localization, and dense features,” *arXiv preprint arXiv:2502.14786*, 2025.
- [19] J. Wang, M. Chen, N. Karaev, A. Vedaldi, C. Rupprecht, and D. Novotny, “Vggt: Visual geometry grounded transformer,” in *Proceedings of the Computer Vision and Pattern Recognition Conference*, 2025, pp. 5294–5306.
- [20] D. Zhuo, W. Zheng, J. Guo, Y. Wu, J. Zhou, and J. Lu, “Streaming 4d visual geometry transformer,” *arXiv preprint arXiv:2507.11539*, 2025.
- [21] S. Yuan, Y. Yang, X. Yang, X. Zhang, Z. Zhao, L. Zhang, and Z. Zhang, “Infinitevgg: Visual geometry grounded transformer for endless streams,” *arXiv preprint arXiv:2601.02281*, 2026.
- [22] Q. Wang, Y. Zhang, A. Holynski, A. A. Efros, and A. Kanazawa, “Continuous 3d perception model with persistent state,” in *Proceedings of the Computer Vision and Pattern Recognition Conference*, 2025, pp. 10 510–10 522.
- [23] D. Wu, F. Liu, Y.-H. Hung, and Y. Duan, “Spatial-mlm: Boosting mllm capabilities in visual-based spatial intelligence,” 2025, *arXiv:2505.23747*.
- [24] Z. Fan, J. Zhang, R. Li, J. Zhang, R. Chen, H. Hu, K. Wang, H. Qu, D. Wang, Z. Yan, H. Xu, J. Theiss, T. Chen, J. Li, Z. Tu, Z. Wang, and R. Ranjan, “Vlm-3r: Vision-language models augmented with instruction-aligned 3d reconstruction,” 2025, *arXiv:2505.20279*.
- [25] F. Li, W. Song, H. Zhao, J. Wang, P. Ding, D. Wang, L. Zeng, and H. Li, “Spatial forcing: Implicit spatial representation alignment for vision-language-action model,” 2025, *arXiv:2510.12276*.
- [26] S. Zeng, D. Qi, X. Chang, F. Xiong, S. Xie, X. Wu, S. Liang, M. Xu, and X. Wei, “Janusvln: Decoupling semantics and spatiality with dual implicit memory for vision-language navigation,” 2025, *arXiv:2509.22548*.
- [27] J. Krantz, A. Gokaslan, D. Batra, S. Lee, and O. Maksymets, “Waypoint models for instruction-guided navigation in continuous environments,” in *Proceedings of the IEEE/CVF International Conference on Computer Vision*, 2021, pp. 15 162–15 171.
- [28] Y. Hong, Z. Wang, Q. Wu, and S. Gould, “Bridging the gap between learning in discrete and continuous environments for vision-and-language navigation,” in *Proceedings of the IEEE/CVF conference on computer vision and pattern recognition*, 2022, pp. 15 439–15 449.
- [29] J. Krantz and S. Lee, “Sim-2-sim transfer for vision-and-language navigation in continuous environments,” in *European conference on computer vision*. Springer, 2022, pp. 588–603.
- [30] Z. Wang, X. Li, J. Yang, Y. Liu, and S. Jiang, “Gridmm: Grid memory map for vision-and-language navigation,” in *Proceedings of the IEEE/CVF International conference on computer vision*, 2023, pp. 15 625–15 636.
- [31] D. An, H. Wang, W. Wang, Z. Wang, Y. Huang, K. He, and L. Wang, “Etpnav: Evolving topological planning for vision-language navigation in continuous environments,” *IEEE Transactions on Pattern Analysis and Machine Intelligence*, 2024.
- [32] Y. Long, W. Cai, H. Wang, G. Zhan, and H. Dong, “Instructnav: Zero-shot system for generic instruction navigation in unexplored environment,” *arXiv preprint arXiv:2406.04882*, 2024.
- [33] K. Chen, J. K. Chen, J. Chuang, M. Vázquez, and S. Savarese, “Topological planning with transformers for vision-and-language navigation,” in *Proceedings of the IEEE/CVF Conference on Computer Vision and Pattern Recognition*, 2021, pp. 11 276–11 286.
- [34] Z. Wang, X. Li, J. Yang, Y. Liu, and S. Jiang, “Sim-to-real transfer via 3d feature fields for vision-and-language navigation,” *arXiv preprint arXiv:2406.09798*, 2024.
- [35] Z. Yu, Y. Long, Z. Yang, C. Zeng, H. Fan, J. Zhang, and H. Dong, “Correctnav: Self-correction flywheel empowers vision-language-action navigation model,” *arXiv preprint arXiv:2508.10416*, 2025.
- [36] Y. Liu, K. Zhang, Y. Li, Z. Yan, C. Gao, R. Chen, Z. Yuan, Y. Huang, H. Sun, J. Gao *et al.*, “Sora: A review on background, technology, limitations, and opportunities of large vision models,” *arXiv preprint arXiv:2402.17177*, 2024.
- [37] X. Zhou, D. Liang, S. Tu, X. Chen, Y. Ding, D. Zhang, F. Tan, H. Zhao, and X. Bai, “Hermes: A unified self-driving world model for simultaneous 3d scene understanding and generation,” in *Proceedings of the IEEE/CVF International Conference on Computer Vision*, 2025, pp. 27 817–27 827.
- [38] C. Dang, H. Liu, J. Bao, P. An, X. Tang, J. Ma, B. Sun, Y. Wang *et al.*, “Sparseworld: A flexible, adaptive, and efficient 4d occupancy world model powered by sparse and dynamic queries,” *arXiv preprint arXiv:2510.17482*, 2025.
- [39] J. Yang, S. Yang, A. W. Gupta, R. Han, L. Fei-Fei, and S. Xie, “Thinking in space: How multimodal large language models see, remember, and recall spaces,” in *Proceedings of the Computer Vision and Pattern Recognition Conference*, 2025, pp. 10 632–10 643.
- [40] S. Yang, J. Yang, P. Huang, E. Brown, Z. Yang, Y. Yu, S. Tong, Z. Zheng, Y. Xu, M. Wang *et al.*, “Cambrian-s: Towards spatial supersensing in video,” *arXiv preprint arXiv:2511.04670*, 2025.
- [41] B. Kerbl, G. Kopanas, T. Leimkühler, G. Drettakis *et al.*, “3d gaussian splatting for real-time radiance field rendering,” *ACM Trans. Graph.*, vol. 42, no. 4, pp. 139–1, 2023.
- [42] X. Chen, Y. Chen, Y. Xiu, A. Geiger, and A. Chen, “Tt3r: 3d reconstruction as test-time training,” *arXiv preprint arXiv:2509.26645*, 2025.
- [43] I. Ahmed, S. Islam, P. P. Datta, I. Kabir, N. U. R. Chowdhury, and A. Haque, “Qwen 2.5: A comprehensive review of the leading resource-efficient llm with potential to surpass all competitors,” *Authorea Preprints*, 2025.
- [44] P. Anderson, Q. Wu, D. Teney, J. Bruce, M. Johnson, N. Sünderhauf, I. Reid, S. Gould, and A. Van Den Hengel, “Vision-and-language navigation: Interpreting visually-grounded navigation instructions in real environments,” in *Proceedings of the IEEE conference on computer vision and pattern recognition*, 2018, pp. 3674–3683.
- [45] A. Ku, P. Anderson, R. Patel, E. Ie, and J. Baldridge, “Room-across-room: Multilingual vision-and-language navigation with dense spatiotemporal grounding,” in *Proceedings of the 2020 Conference on Empirical Methods in Natural Language Processing (EMNLP)*, 2020, pp. 4392–4412.
- [46] H. Tan, L. Yu, and M. Bansal, “Learning to navigate unseen environments: Back translation with environmental dropout,” in *Proceedings of the 2019 Conference of the North American Chapter of the Association for Computational Linguistics: Human Language Technologies, Volume 1 (Long and Short Papers)*, 2019, pp. 2610–2621.
- [47] S. Ross, G. Gordon, and D. Bagnell, “A reduction of imitation learning and structured prediction to no-regret online learning,” in *Proceedings of the fourteenth international conference on artificial intelligence and statistics*. JMLR Workshop and Conference Proceedings, 2011, pp. 627–635.
- [48] S. K. Ramakrishnan, A. Gokaslan, E. Wijmans, O. Maksymets, A. Clegg, J. Turner, E. Undersander, W. Galuba, A. Westbury, A. X. Chang *et al.*, “Habitat-matterport 3d dataset (hm3d): 1000 large-scale 3d environments for embodied ai,” *arXiv preprint arXiv:2109.08238*, 2021.
- [49] Z. Wang, J. Li, Y. Hong, Y. Wang, Q. Wu, M. Bansal, S. Gould, H. Tan, and Y. Qiao, “Scaling data generation in vision-and-language navigation,” in *Proceedings of the IEEE/CVF international conference on computer vision*, 2023, pp. 12 009–12 020.
- [50] Y. Zhang, J. Wu, W. Li, B. Li, Z. Ma, Z. Liu, and C. Li, “Video instruction tuning with synthetic data, 2024,” URL <https://arxiv.org/abs/2410.02713>, vol. 17.
- [51] D. Azuma, T. Miyanishi, S. Kurita, and M. Kawanabe, “Scanqa: 3d question answering for spatial scene understanding,” in *proceedings of the IEEE/CVF conference on computer vision and pattern recognition*, 2022, pp. 19 129–19 139.
- [52] J. Krantz, E. Wijmans, A. Majumdar, D. Batra, and S. Lee, “Beyond the nav-graph: Vision-and-language navigation in continuous environments,” in *European Conference on Computer Vision (ECCV)*. Springer, 2020, pp. 104–120.
- [53] S. Raychaudhuri, S. Wani, S. Patel, U. Jain, and A. Chang, “Language-aligned waypoint (law) supervision for vision-and-language navigation in continuous environments,” in *Proceedings of the 2021 conference on empirical methods in natural language processing*, 2021, pp. 4018–4028.
- [54] G. Georgakis, K. Schmeckpeper, K. Wanchoo, S. Dan, E. Mitsakaki, D. Roth, and K. Daniilidis, “Cross-modal map learning for vision and language navigation,” in *Proceedings of the IEEE/CVF Conference on Computer Vision and Pattern Recognition (CVPR)*, June 2022, pp. 15 460–15 470.
- [55] P. Chen, D. Ji, K. Lin, R. Zeng, T. Li, M. Tan, and C. Gan, “Weakly-supervised multi-granularity map learning for vision-and-language navigation,” *Advances in Neural Information Processing Systems*, vol. 35, pp. 38 149–38 161, 2022.